


Article

# Managing Power Demand from Air Conditioning Benefits Solar PV in India Scenarios for 2040<sup>†</sup>

Ahmad Murtaza Ershad<sup>1,2,\*</sup>, Robert Pietzcker<sup>1</sup>, Falko Ueckerdt<sup>1</sup> and Gunnar Luderer<sup>1,2</sup>

<sup>1</sup> Potsdam Institute for Climate Impact Research, PO Box 601203, 14412 Potsdam, Germany; pietzcker@pik-potsdam.de (R.P.); ueckerdt@pik-potsdam.de (F.U.); luderer@pik-potsdam.de (G.L.)

<sup>2</sup> Global Energy System Analysis, Technical University of Berlin, 10623 Berlin, Germany

\* Correspondence: ershad@pik-potsdam.de; Tel.: +49-331-288-2549

<sup>†</sup> An early draft of this paper was presented at the 2nd International Conference on Large-Scale Grid Integration of Renewable Energy in India and published in the conference's proceedings.

Received: 6 March 2020; Accepted: 18 April 2020; Published: 2 May 2020



**Abstract:** An Indian electricity system with very high shares of solar photovoltaics seems to be a plausible future given the ever-falling solar photovoltaic (PV) costs, recent Indian auction prices, and governmental support schemes. However, the variability of solar PV electricity, i.e., the seasonal, daily, and other weather-induced variations, could create an economic barrier. In this paper, we analyzed a strategy to overcome this barrier with demand-side management (DSM) by lending flexibility to the rapidly increasing electricity demand for air conditioning through either precooling or chilled water storage. With an open-source power sector model, we estimated the endogenous investments into and the hourly dispatching of these demand-side options for a broad range of potential PV shares in the Indian power system in 2040. We found that both options reduce the challenges of variability by shifting electricity demand from the evening peak to midday, thereby reducing the temporal mismatch of demand and solar PV supply profiles. This increases the economic value of solar PV, especially at shares above 40%, the level at which the economic value roughly doubles through demand flexibility. Consequently, DSM increases the competitive and cost-optimal solar PV generation share from 33–45% (without DSM) to ~45–60% (with DSM). These insights are transferable to most countries with high solar irradiation in warm climate zones, which amounts to a major share of future electricity demand. This suggests that technologies, which give flexibility to air conditioning demand, can be an important contribution toward enabling a solar-centered global electricity supply.

**Keywords:** renewable electricity integration; market value; wind and solar PV; demand-side management; air conditioning; India; power sector modelling

## 1. Introduction

Several drivers make the transition of the Indian electricity system toward high shares of solar photovoltaics (solar PV) a plausible future: (i) The falling solar PV capacity costs as reflected in recent Indian renewable electricity auction prices (37 USD per MWh [1]), (ii) government ambitions to ramp up renewable energy generation capacity to 500 GW by 2030 from 175 GW planned by 2022 [2], and (iii) the potential future role indicated by scenario results from global and national energy-economic models [3–6]. Using scenario data from six global models and limiting global warming to 2 °C, McCollum et al. [6] showed that the share of global low-carbon supply-side investments in the total supply-side investments has to reach 80% by 2050. For India, the share of solar generation in the final electricity demand has to reach levels of up to 66% in order to limit global warming to 2 °C by 2050.

However, a potential barrier to the transition to such a sustainable future are challenges related to the variability of solar PV generation [7], i.e., the seasonal, daily, and weather-induced variation of solar PV output. These physical and technical properties translate into mostly adverse economic impacts. Analytical, empirical, and modeling evidence shows that as the share of solar PV electricity in the total electricity demand increases, its economic value to the system decreases due to variability and, mostly, the temporal mismatch of solar PV supply and demand, especially in a system with only limited flexibility options [8–10]. In functioning power markets, the decrease in economic value translates to a decrease of the average price paid for electricity produced by a PV plant—also called PV market value or value of solar (VOS).

This decline has serious implications for the achievement of high solar shares, as it affects the profitability of solar investments, as well as total electricity system costs. The phenomenon of solar devaluation at higher shares has been well studied for developed power systems such as California [11], Germany [12], Italy [13], and Florida [14]. India-specific studies on the challenges and opportunities of high variable renewable energy (VRE) penetration levels are available in the grey literature [15–17], but there is still demand for more scientific publications on this topic.

A number of innovative strategies have been explored for integrating variable generation from solar PV, including shifting of electricity demand in time [18], deploying batteries [19,20], building integrated photovoltaics (BIPV) [21] and their coupling with micro-wind turbines [22], electrification of programmable consumption of private transport and space heating [23], solar PV output-shaping to align with wholesale electricity price profiles [24], and conversion of electrical power to heat using heat pumps and thermal storage [25,26].

For India, a promising DSM measure to mitigate the decline in the market value of solar PV generation is to make AC demand flexible with cool thermal energy storage (CTES) [27,28]. Electricity demand for space cooling with air conditioners (AC demand) is expected to increase significantly in the future, particularly in high-temperature countries like India due to increasing household income, urbanization and global warming [29–31], which will pose significant power challenges such as an increased need for expensive peaking power plants [32–35]. Thus, AC demand flexibility will meet both the need to integrate solar PV generation and reduce investments in peaking plants.

There are various CTES technologies with various performance characteristics and costs that can shift AC demand, including mechanical precooling the building thermal mass [36–39], chilled water or ice storage technologies [40–43], and phase change material such as hydrated salts [44]. Traditionally, AC demand flexibility measures have been exploited to shift AC demand to off-peak periods when electricity rates are low. Through these measures, peak demand is reduced by either advancing cooling energy a few hours during the day or shifting cooling energy to nighttime to chill water, make ice, or ventilate the building, benefiting from lower outside temperatures.

The use of AC demand with CTES to improve the mismatch between variable generation and electricity demand in addition to reducing peak demand has gained some attention [45–47] due to growth of variable generation. Van Asselt et al. [45] proposed a strategy to maximize a single building's utilization of renewable electricity using a single storage tank holding stratified water. In the proposed strategy, renewable power (solar and wind) was utilized by the system chillers at all times unless renewable power dropped below the chiller minimum part-load ratio. Deetjen et al. [46] used CTES as part of a residential central utility plant that also included batteries, a microturbine, and a chiller to address grid operational difficulties due to solar PV generation. The dispatch and investment of the CUP was optimized using different exogenous electricity rate structures. They found that when solar PV did not exceed demand, CTES improved chiller operation and reduced net peak demand by charging during the night and early morning and discharging during net peak demand. However, when solar generation exceeded demand, CTES charged during the early afternoon and discharged during the net peak demand, thus reducing curtailment and net peak demand. Goldenberg et al. [47] analyzed the impact of several demand response measures—including AC-based demand flexibility via ice storage—on the wholesale electricity market in Texas, ERCOT, in 2050. Ice storage systems were

modeled to store cooling energy in ice during the hours with the lowest net load (total load minus generation from solar and wind) and discharge during the hours with the highest net load. They found that electric vehicles provided a large share of the demand response at low costs, and ice storage AC demand response provided the second largest share, but at substantially higher costs. However, their analysis was limited to one scenario with a relatively low PV and medium wind share of 18% and 42%, respectively, and did not detail the changes in revenues for PV plants specifically.

In this study, we used the open-source power sector model DIETER [48] to explore the potential of two AC-related demand side management options to facilitate the integration of solar PV in the Indian electricity system in 2040. We investigated the impact of precooling and chilled water storage on the economic value of solar PV and the resulting cost-optimal share of PV in the generation mix. We acknowledge the large uncertainties surrounding many input parameters due to technology and demand evolution, given that our analysis was concerned with a situation 20 years in the future. Accordingly, the focus of our analysis was not on determining exact values, but rather on estimating the type and rough magnitude of effects that either a short-period demand response option (precooling) or a longer-period demand response option (chilled water storage) can have on a future Indian power system and the challenge of PV integration.

## 2. Methodology

The flowchart (Figure 1) shows our methodology, i.e., the four main steps we took to estimate the impact of DSM on solar PV market values. These four steps are described in the four subsections of this methodology section. We first defined three scenarios that allowed us to compare the two DSM measures (precooling and CWS) with a reference case (*noDSM*) (Section 2.1). Second, we described the relevant data, parameter, and crucial assumptions, which were input to the numerical model (Section 2.2). Inputs include hourly AC and overall electricity demand, hourly demand, solar, wind and hydro generation profiles, fuel and CO<sub>2</sub> prices, and cost and performance characteristics of generation and DSM technologies. Then, we introduced the methodological core of our analysis: The open-source power sector investment and dispatch model DIETER (Section 2.3), with which we explored three scenarios of managing AC electricity demand. The main outputs of the DIETER model include the investments into and dispatching patterns of all power generation and DSM technologies, as well as overall electricity prices (Section 2.3). For the three scenarios and for a broad range of exogenous solar PV shares, DIETER endogenously adjusts capacity and operation of the power system, including generation and, particularly, DSM technologies. Finally, we conducted postprocessing and analyses based on the model outputs across scenarios (Section 2.4). Most importantly, using endogenous electricity prices from DIETER, we calculated the market value of solar PV generation, the expected levelized cost of electricity from solar PV plants, and an estimate of the cost-efficient shares of solar PV investments with and without DSM.

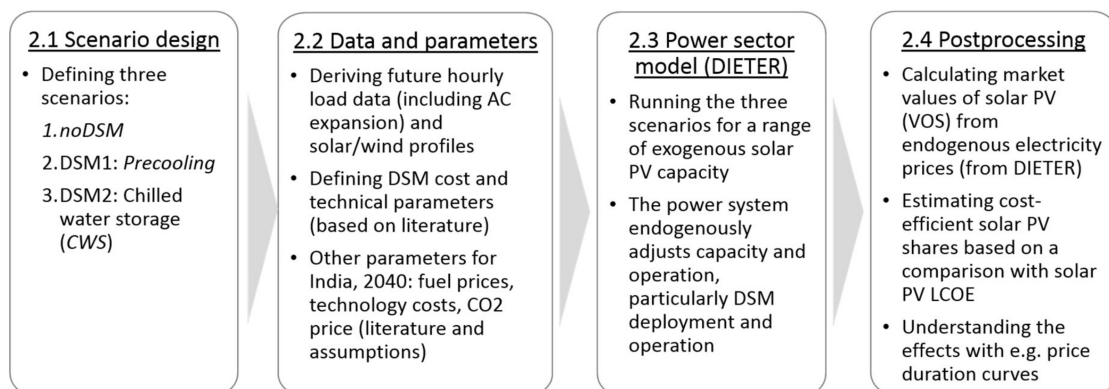


Figure 1. Modeling and analysis flow diagram.

## 2.1. Scenario Design

We explored three scenarios of managing AC electricity demand in a highly air-conditioned Indian electricity system in 2040. In all three scenarios, air conditioning made up 23% of the total electricity demand, in accordance with Levesque et al. (2017), and the peak AC demand was 350 GW (see Appendix A for information about the electricity demand calculations).

In the first scenario, *noDSM*, we assumed inflexible AC demand that did not react to electricity prices. This method of AC operation is the current default [49] and serves as a reference scenario to evaluate the value of flexibility of DSM. In this scenario, the temporal profile of AC demand closely corresponds to outdoor temperatures with some delay due to building thermal insulation and thermal mass.

In the second scenario, *Precooling*, AC demand was capable of responding to electricity prices with the help of a programmable thermostat. This is a rather short-period demand response option. The building's thermal mass functions as a storage medium to store cooling energy during low-price hours and release it when prices increase. Whereas shifting AC demand by precooling is a very simple measure that is easy to implement, the impact is limited as humans' thermal comfort zone limits both the maximum cooling energy that can be stored, as well as the charge/discharge period. When cooling energy is stored in the building, room temperatures are below the point deemed comfortable by inhabitants. The optimal temperature range is one of the many user experience considerations of a number of field trials testing the deployment of precooling to reduce peak demand [50]. In this scenario, the only additional cost was the investment to replace conventional thermostats with programmable thermostats.

In the third scenario, the *CWS* scenario, AC demand could also react to electricity prices, but in this case, the shifting was enabled through the operation of cool thermal energy systems, namely chilled water storage (CWS) tanks. The installation of CWS tanks comes with higher cost than just the programmable thermostat in *Precooling*, but provides greater flexibility as more cooling energy can be stored, and the charge/discharge period can be longer.

DSM provision in *Precooling* and *CWS* varies with respect to investment cost, maximum DSM duration, and round-trip efficiency (Table 1). Precooling represents a very low-cost DSM measure that only requires equipping all buildings with a programmable thermostat [36], but it has its limitations. As previously mentioned, the thermal comfort of building occupants is affected by the necessity to overcool the space. Moreover, storing cold air in the building's thermal mass is neither very efficient, nor does it allow for the temporal decoupling of the charging (cooling) period from the discharge (return to desired temperatures) period, since doing so would increase the time in which the occupants have to endure cooler-than-desired room temperatures. CWS mitigates the above limitations, as the water storage tank removes the inconvenience of overcooling and decouples charging from discharging for extended periods. However, chilled water storage tanks have higher investment costs and require space [45], which would be a constraint for some Indian buildings.

**Table 1.** Main assumptions of our demand-side management (DSM) scenarios.

DSM Parameter	Scenarios			Unit
	noDSM (Reference Scenario: No Flexibility for Shifting Exogenous AC Demand)	Precooling (Only DSM Option 1)	CWS (Only DSM Option 2)	
Overnight investment costs	/	30	100	USD/kW
Round-trip Efficiency	/	70	90	%
Maximum DSM duration	/	4	8	Hours

## 2.2. Data and Parameters

Here, we discuss the data, parameters, and assumptions that are the main inputs to the economic modeling with the DIETER model, which is described in the next section. As a basis for the DIETER model, we projected the annual electricity demand and the future AC share for India in 2040 (Table 2). Based on projections by Levesque et al. (2019) [51], for the noDSM scenario, we assumed an AC electricity demand of 807 TWh and a total electricity demand of 3537 TWh for India in 2040. To compare, total electricity demand in 2010 was ~770 GWh [52]. The share of AC demand in total electricity demand is projected to increase from around 8% in 2010 to around 22% in 2040.

**Table 2.** Electricity demand (baseline and 2040).

Parameter	Year 2010	Year 2040	Unit
Total load	769	3535	TWh
Total AC demand	57	807	TWh
Load factor (%)	84	67	%
Peak load (GW)	105	606	GW
Average load (GW)	88	403	GW
Minimum load (GW)	66	259	GW
Maximum peak-coincident AC demand (GW)	25	350	GW
Time of total peak load	8:00 PM	5:00 PM	
Month of peak load	October	May	

To derive the hourly profile of total electricity demand in a highly air-conditioned India in 2040, we used a partial disaggregation approach similar to Boßmann et al. [53], focusing on the effect of the increase in AC's share of demand on the hourly profile without assuming changes in other demand categories. Thus, the projected electricity demand curve captured the increase in AC demand, which peaked early in the evening. To ground our projections to empirical observations, we first estimated the hourly AC demand profile in 2010 using an extended degree-day method. Next, we disaggregated the 2010 total electricity demand profile into AC and non-AC demand, scaled each using their distinct growth rates to match the 2040 total electricity demand and the split given by Levesque et al. (2019), and summed the new rescaled profiles to arrive at the final 2040 hourly total electricity demand profile. The details of this procedure can be found in the appendix.

Hourly solar PV generation profile in MWh per MW of installed capacity for eight Indian state capitals that have the highest utility scale solar PV potential as estimated by U.S. National Renewable Energy Laboratory (NREL) [54] was simulated using NREL's System Analysis Model (SAM 2017.1.17) [55] and averaged to represent hourly solar PV yield for India. Assumptions for the technical specification of PV plants considered in this study are the same as those described by the authors of [54]. Hourly solar PV yield for India was computed as a weighted average of hourly solar PV yield based on the potential of solar PV deployment in each of the eight states as estimated by the authors of [54] under the scenario of installing 60 GW of PV in India by 2022.

The hourly wind generation profile in MWh per MW of installed capacity was simulated using Renewables.ninja (<https://www.renewables.ninja/>), an online simulator of hourly wind power plant output. Table A1 in the appendix documents the locations of assumed wind farms for the calculation of hourly wind power yield in MWh per MW taken from <https://www.thewindpower.net/>. We simulated wind power output for a Suzlon S97 2100 wind turbine at a hub height of 100 m using the MERRA-2 (global) dataset for 2010. Based on our modeling, we estimated annual solar and wind capacity factors to be 20% and 31%, respectively.

For all scenarios, we assumed a CO<sub>2</sub> price of 50 USD/tCO<sub>2</sub> to represent a setting in which India implements a climate policy of medium stringency. We contend that this value falls within a plausible range for 2040, as Indian policymakers have formulated their intent of limiting climate change in

accordance with the Paris Agreement, but have also expressed that economic growth is a priority given its status as developing country.

Whereas the model can endogenously build hard coal, combined cycle gas, and combustion turbines, as well as nuclear power plants to meet the electricity demand in all scenarios, we assume a number of bounds on maximum/minimum capacities to represent limitations on resource potential, existing capacities or scale-up speeds:

- 20 GW of pumped hydro storage with 4 h of storage capacity and 40 GW of hydro capacity with a constant capacity factor of 35%. This amount of total hydro capacity (60 GW) is consistent with estimates of installed capacity of hydro by IEA WEO 2018 New Policies Scenario (NPS) for the next five years in India. Our assumption that hydro capacity will not grow in the next decades is consistent with the finding by Lawrenz et al. [3] that hydro capacity will stay almost constant between 2015 and 2050. Pumped hydro storage is dispatched endogenously, while the rest of the hydro capacity is available for dispatch at a constant capacity factor of 35% at all hours of the year, consistent with annual average hydro capacity factor reported by the authors of [56].
- A wind capacity of 209 GW, equivalent to 11% of wind electricity in final electricity demand, consistent with the IEA WEO 2018 New Policies Scenario (NPS)
- A minimum of 147 GW of standing hard coal capacity in 2040 to reflect the current heavy reliance of India on coal on one hand and the potential coal-phase out on the other.
- A maximum capacity limit of 47 GW for nuclear. This value is the maximum value for India in the 2018 IEA WEO scenarios, and seems very ambitious given the historically long build times of nuclear power plants in India, as well as the fact that the government target for 2031 is only 22 GW [57].
- Our assumptions about the 2040 technology parameters, fuel, and CO<sub>2</sub> prices were derived by assessing and combining information in [15,58–64] and are described in Tables A2 and A3 in the Appendix B.

### 2.3. Power Sector Model (DIETER)

With the open-source power sector investment and dispatch model DIETER [65], we explored the three scenarios of managing AC electricity demand. The main outputs of the DIETER model include investments into and dispatch of generation and DSM technologies, as well as electricity prices. The scenarios were calculated based on the above assumptions and a broad range of exogenously defined solar PV shares in electricity generation.

DIETER is a partial equilibrium model of the wholesale electricity market, focusing on both the supply and the demand side. DIETER minimizes total system costs over 8760 h of a full year, ensuring that power generation equals demand at all times. In its basic formulation, system costs comprise annualized investment costs, fixed operation and maintenance costs, and variable costs of dispatchable power generators (e.g., fuel and CO<sub>2</sub> costs), variable renewables, and demand-side management (DSM) technologies. We used the marginal of the demand balance equation, which represents the shadow price of hourly demand as a proxy for wholesale electricity prices. The resulting prices can be interpreted as the prices of an energy-only market with scarcity pricing in which all capacity investments can be recovered through revenues from electricity sales.

To implement the DSM technologies above defined in the model, we built upon a wholesale DSM model formulation suggested by the authors of [66], called here AC-DSM, which allowed different DSM technologies (*ls*) to participate in the wholesale electricity market. The main AC-DSM inputs (Table A4) include DSM investment and operation costs, DSM technical lifetime and efficiency, maximum DSM duration, maximum DSM installed capacity, recovery period between two DSM cycles, and an hourly AC demand profile. The most important outputs are the optimal DSM installed capacity and hourly wholesale load addition and reduction. In the following, the main equations used in the formulation of AC-DSM are explained.

As neither DSM measure is currently widely used in India, exact cost numbers were not available. Inferring from other regions, we assumed that, in the Precooling scenario, a programmable thermostat would cost about 30 USD per unit and that, by installing one, households could save 1 kW of electricity. We assumed that a programmable thermostat was capable of shifting the full electrical power consumption of a single-room AC unit. One kilowatt was our estimate for electrical power consumption of a typical room AC unit in India in 2040. This is consistent with the assumption of Phadke et al. [35], assuming 1.5 kW of electrical power consumption for a room AC unit in India in 2030. At present, in April 2020, one can purchase a programmable thermostat manufactured by Honeywell for \$30 USD. In the CWS scenario, we assumed that a chilled water storage system with an 8-h tank would cost 100 USD per kW of AC electricity demand. This assumption for 2040 is consistent with the lowest range of current CTES power costs (100–1100 USD per kW) reported by Van Asselt et al. (2017) [45].

AC demand can be increased or decreased at any time during the day. However, each unit of electricity increased is decreased no later than the maximum shift duration accounting for efficiency. Maximum shift durations were assumed to be 4 h and 8 h in the *Precooling* and *CWS* scenarios, respectively. The amount of cooling energy that can be stored during low-price hours depends on how soon the stored energy is discharged. In the *Precooling* scenario, stored energy was discharged within 4 h. This means that, a fully cooled room at 10 a.m. would return to ambient temperatures by 2 p.m. Using chilled water tanks allowed us to increase this period to 8 h in the *CWS* scenario. This allowed for more flexibility in demand shifting.

AC-DSM always shifts AC demand to an earlier time. In other words, the model first increases AC demand when prices are low to either precool the building thermal mass or lower the temperature of water in the chilled water tank. The model then reduces system load in the subsequent hours to account for loads increased in previous hours, after correcting for process inefficiencies ( $\varepsilon_{ls}$ ) (1). The increased load in an hour has to be balanced within the maximum DSM duration ( $t_{ls}^{dur}$ ).

$$DSM_{ls,h}^{UP} \varepsilon_{ls} = \sum_{h \leq hh \leq h + t_{ls}^{dur}} DSM_{ls,h, hh}^{DOWN} \quad (1)$$

The total wholesale load reduction in an hour cannot be larger than the DSM installed capacity ( $N_{ls}$ ) multiplied by the hourly AC profile ( $\varphi_{AC}$ ) (2). Including a temporal profile for the DSM installed capacity replicates the fact that not all AC units participating in the DSM program are turned on at every hour due to occupancy or temperature constraints.

$$DSM_{ls,h}^{DOWN} \leq \varphi_{AC} N_{ls} \quad (2)$$

In addition, total wholesale load addition in an hour cannot be larger than the difference between the maximum DSM capacity and the total wholesale reduction (3).

$$DSM_{ls,h}^{UP} \leq 1.2 N_{ls} - \varphi_{AC} N_{ls} \quad (3)$$

We made two assumption in the above equation. First, we assumed the DSM installed capacity to be 80% of the maximum DSM installed capacity. In other words, we assumed that not all ACs participating in the DSM program were operating at maximum capacity, and that their consumption could be increased to the maximum capacity when DSM is economically viable. Second, we assumed that all ACs participating in the DSM program were available to be turned on whenever called upon. This is no problem if buildings are not occupied. However, if buildings are occupied, it might hamper thermal comfort.

Finally, we limited the DSM installed capacity ( $N_{ls}$ ) to a fixed exogenous capacity limit ( $m_{ls}$ ), which was the overall peak AC demand seen in the power system (4). We assumed that the electricity

consumption of all of the air conditioners turned on in the peak hour was available to be shifted to an earlier time.

$$N_{Is} = m_{Is} \quad (4)$$

In our scenarios, we assumed that all of the projected AC demand was available to be shifted, allowing us to estimate an upper limit to the potential effect of AC-based demand response. In reality, the share of participating ACs will likely be lower, as not all occupants will be willing to precool their apartment, and some buildings may not have enough space to install a chilled water tank.

#### 2.4. Postprocessing

We estimated VOS by dividing the total wholesale revenues of solar plants by the total gross solar generation (“gross” meaning “generation before curtailment”) (5). Wholesale solar revenues were estimated by summing the product of wholesale electricity prices and solar feed-in over all the hours of the year. Here, we assumed all solar plants to be utility-scale and that these plants sell their generated electricity at the wholesale electricity price. The approach captures both the energy value and the capacity value since the wholesale price model includes scarcity pricing.

$$\text{value of solar} = \frac{\sum_{h=1}^{8760} P_h G_{PV}}{\left(\sum_{h=1}^{8760} G_{PV} + \sum_{h=1}^{8760} CU_{PV}\right)} \quad (5)$$

where  $P_h$  is the hourly electricity price,  $G_{PV}$  the solar PV generation sold to the market, and  $CU_{PV}$  the potential solar PV generation that was curtailed.

As a post-processing step, we estimated cost-efficient solar PV shares by comparing the VOS with the expected levelized cost of Electricity (LCOE) of solar PV. The upper value of the LCOE range represents the result of a 2019 solar PV auction in India (37 USD/kWh), the lower value assumes that technology costs are cut in half, resulting in an LCOE of 18 USD/kWh. To help guide the reader’s eye, we added a red line to show the middle value, 27 USD/kWh. We assume that the solar PV LCOE does not change with varying solar PV shares across the scenario runs.

### 3. Results and Interpretations

#### 3.1. Cost-Efficient Solar PV Shares without DSM

In the *noDSM* scenario (Figure 2), we estimated that the VOS would decline from ~90 USD/MWh to less than 10 USD/MWh as the solar PV share increased from 1% to 60%. We estimated cost-efficient solar PV shares to be in the range of ~33–45% for the considered range of assumed 2040 LCOEs for solar PV, ~17–37 USD/MWh. At a solar PV LCOE of ~37 USD/MWh, which was achieved in a 2019 auction [1], and a future AC-heavy demand profile, the cost-efficient share of solar PV would be ~33%. Assuming that the 2040 LCOE of PV would decrease to half the current value due to continued technological learning would increase the cost-efficient share to ~45%. In a functioning market, solar PV plants would thus earn enough revenue to recover their investment costs at PV shares of up to 30–45%.

The reason for this sharp decline is known as the duck curve [14] (Figure 3). The midday residual load significantly dropped with increasing shares of solar PV due to the self-correlation of solar generation (*noDSM* scenario). At 20% share, residual load showed a pronounced evening peak, which could not be shaved by additional solar PV plants (without shifting demand or supply via DSM or electrical storage). Above a 20% solar PV share, PV generation began to exceed electricity demand (on some days of the year; the annual average only exhibits this effect beyond 30%). The average curtailment rates reached ~5% at 30% solar PV share, and ~17% at 40% solar PV share. Note that marginal curtailment rates were even higher.



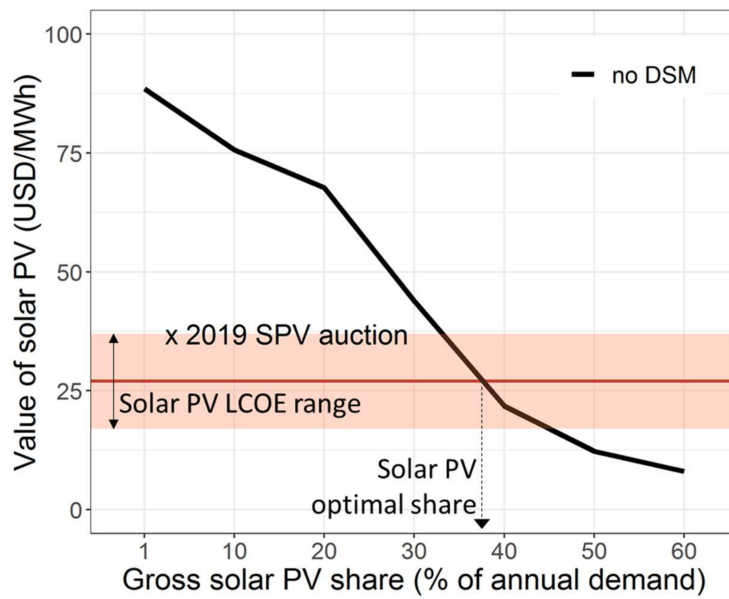


Figure 2. Value of solar (VOS) at different shares of solar PV in the noDSM scenario.

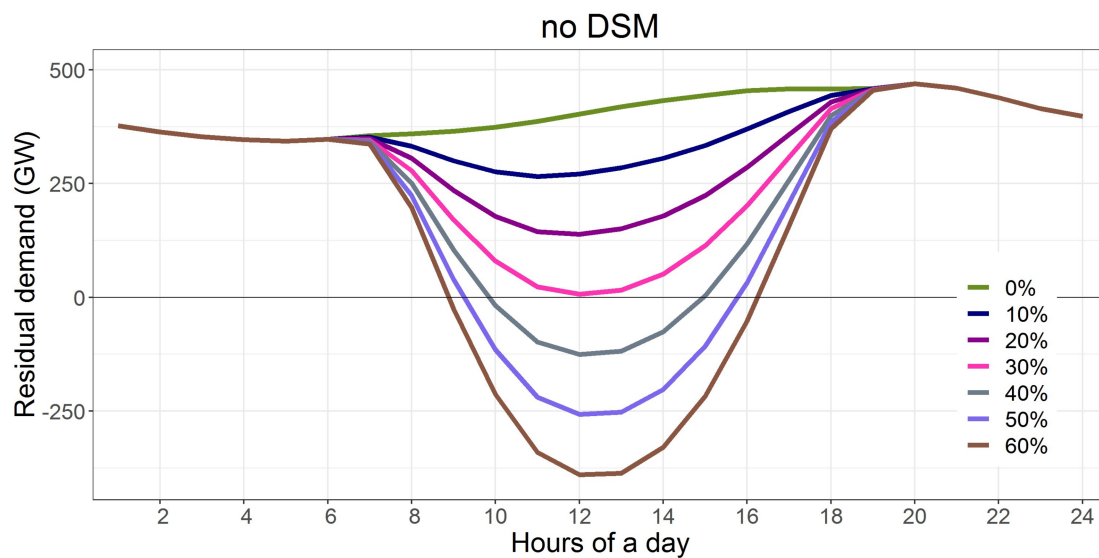
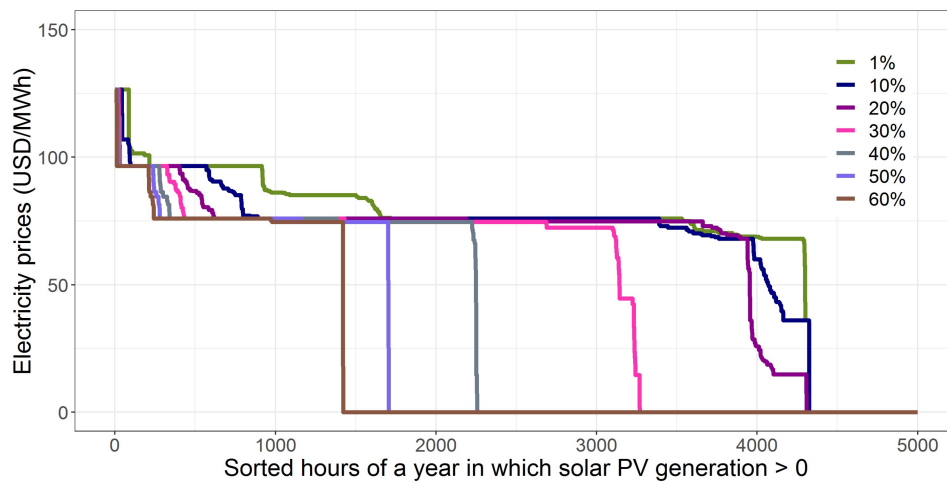


Figure 3. Annual average daily total residual demand for the noDSM scenario. Residual demand was calculated by subtracting gross solar PV generation from total demand.

During the midday dip of residual load, electricity prices declined and resulted in a decline of VOS. Figure 4 shows the price duration for the hours of the year in which solar PV plants were generating, i.e., revenues for solar PV operators. At a 20% share, additional solar generation reduced electricity prices by crowding out more expensive generation capacities (merit order effect) and consequently shifting the electricity price duration curve to the left. Beyond a 20% solar PV share, additional solar generation sometimes exceeded demand and, thus, solar plants became the marginal generator in some hours of the year. Zero-price hours increasingly occurred and average solar PV revenues declined significantly. At a 40% solar PV share in the *noDSM* scenario, ~50% of the solar-PV generating hours faced zero prices.



**Figure 4.** Duration curve of electricity prices for hours with solar PV generation (for different solar PV shares for the noDSM scenario).

### 3.2. Deployment of DSM

In this section, we show modeling results for both of the DSM options. Figure 5 shows how the cost-efficient deployment of each DSM option increased with the share of solar PV. In the *Precooling* scenario, all buildings used the DSM option at just 10% solar PV shares, while, in the *CWS* scenario, this only occurred beginning at a 40% solar share. *CWS* is more expensive and only cost-efficient at higher solar PV shares.

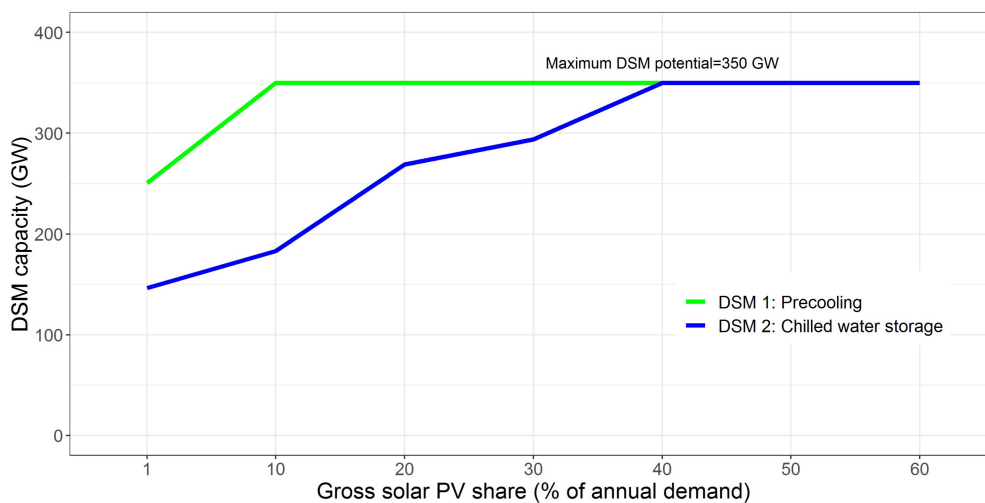


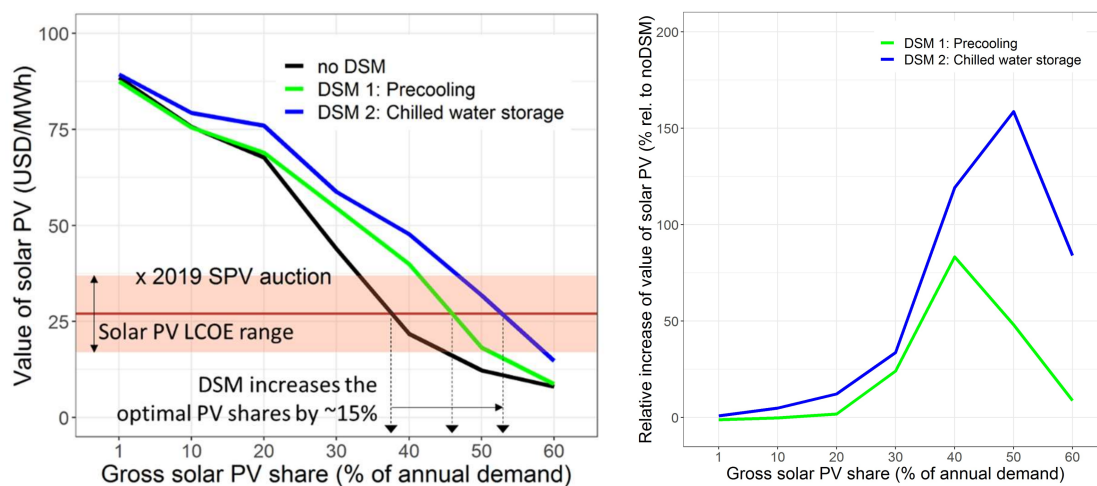
**Figure 5.** Investments in DSM capacity, which determines the converter capacity that is available to shift AC power demand in time. DSM capacity shows AC demand that is available to participate in the wholesale electricity market in the form of CTES power capacity.

This can further be better expressed in relative terms to solar PV capacity. DSM specific capacity started at  $\sim 14$  kW and  $\sim 8$  kW of DSM per kW of solar at 1% PV share in the *Precooling* and *CWS* scenarios, respectively. It quickly dropped to less than 1 kW DSM per kW solar at a 20% PV share and finally reached 0.33 kW DSM per kW solar at a 60% share of PV in both scenarios.

The share of shifted electricity in the total electricity demand in the *CWS* scenario increased with increasing solar share and reached  $\sim 10\%$  at a 60% solar share, while, in the *Precooling* scenario, the highest mark of  $\sim 6\%$  was achieved at 50%. The lower shifting potential of the *Precooling* scenario was due to shorter DSM cycle compared to the *CWS* scenario.

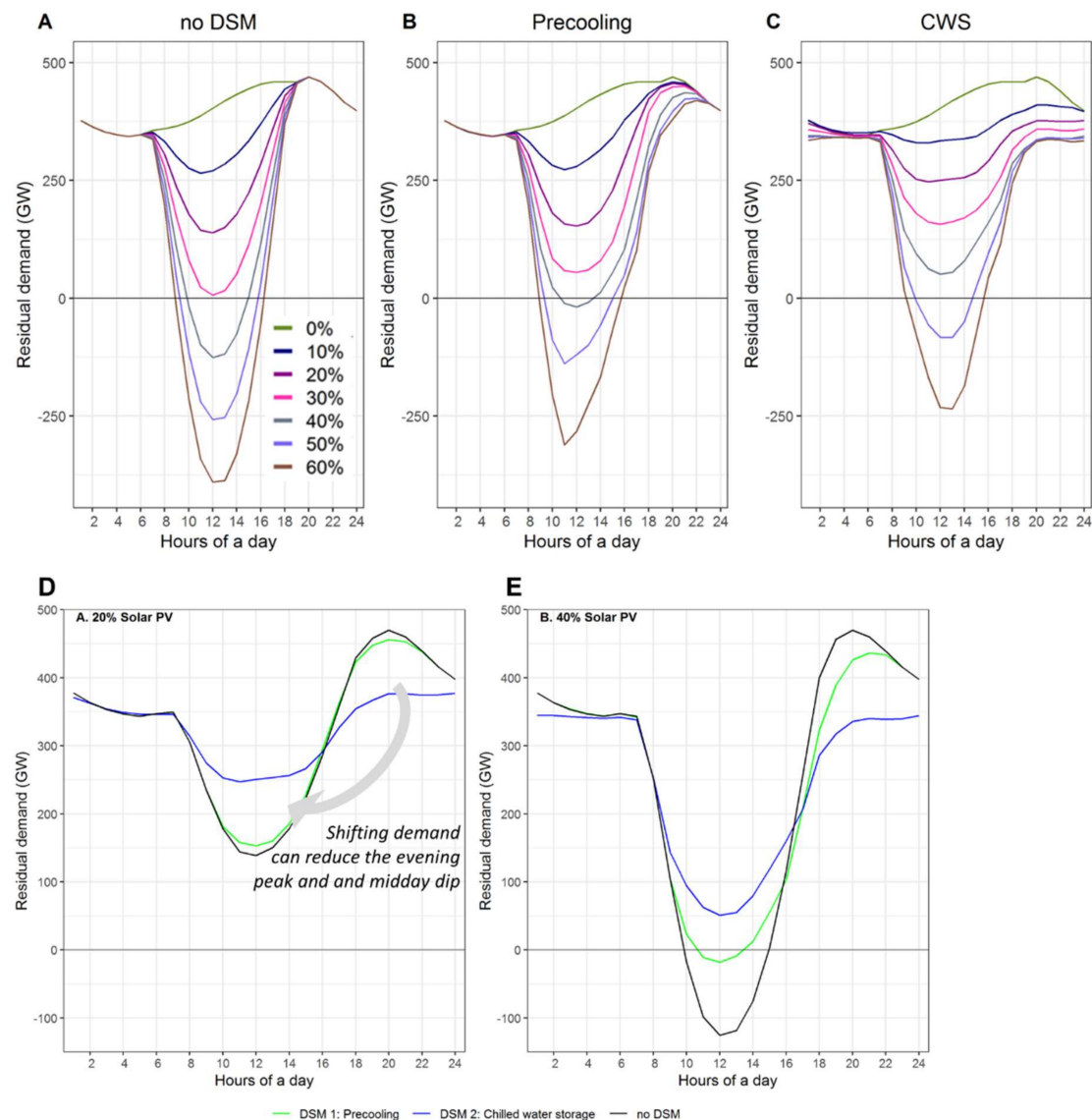
### 3.3. Cost-Efficient Solar PV Shares with DSM

Figure 6 shows the VOS for the *Precooling* and *CWS* scenarios (left) compared to the reference *noDSM* scenario (right). Both options increased the market value of solar PV, particularly when solar PV achieved at least a 20% share in the electricity mix. The cheaper and less flexible option of precooling was less helpful than the more expensive but more flexible *CWS* option. In both cases, the market value could be roughly doubled at a 40% solar share compared to the *noDSM* scenario. Further improvements could only be achieved with greater *CWS* deployment. In absolute terms, precooling increased VOS by 18 USD/MWh at a 40% solar share compared to the *noDSM* scenario. By allowing AC demand to be shifted across a wider time window, *CWS* increased VOS by 26 USD/MWh at a 40% solar share. With CTES shifting AC demand up to 4 h in the *Precooling* scenario, cost-efficient solar shares increased by ~10% compared to the cost-efficient solar shares in the *noDSM* scenario, reaching about 42–52%. Another 5% improvement was achieved by increasing the maximum time-shift to 8 h (*CWS*), increasing cost-efficient solar shares up to ~45–60%.



**Figure 6.** VOS at different solar PV shares in the scenarios with (Precooling and CWS) and without DSM (*noDSM*) (left) and relative increase of VOS compared to the *noDSM* scenario (right).

To understand the load-shifting mechanisms behind the VOS improvements, Figure 7A–C show the hourly residual demand during an average day for all three scenarios. Figure 7A shows the duck curve for the *noDSM* scenario (same as Figure 3). Curtailment decreased for a couple of hours early in the afternoon. Precooling (Figure 7B) slightly shaved the evening peak and flatten the midday dip, while the more flexible *CWS* was capable of completely eliminating the evening peak and significantly reduce the midday dip (Figure 7C). Figure 7D,E show how the DSM options shifted load from the evening peak to midday. At a 20% solar PV share, only *CWS* had the sufficient temporal freedom to flatten the residual load curve. At a 40% solar PV share, there was enough solar generation during early evenings such that precooling could also shave the residual load evening peak to some degree.



**Figure 7.** Annual average daily residual demand for different solar PV shares. Residual demand was calculated by subtracting gross solar PV generation from total electricity demand (electricity demand plus net load change due to DSM). (A–C) show the hourly residual demand during an average day for all three scenarios with increasing solar PV share. (D,E) compares the DSM options for two solar PV generation shares 20% (left) and 40% (right).

Figure 8 shows the electricity price duration curve corresponding to Figure 7D,E. At a 20% solar PV share, solar revenues were slightly increased mostly during a small fraction of hours on the right end of the duration curve. At a 40% solar PV share, solar revenues were significantly increased during what would be zero-price hours in the *noDSM* scenario by reducing solar PV curtailment. Precooling almost entirely resolved the negative portions of residual load (Figure 7D,E) such that the additional benefit of a more flexible DSM option (CWS) were only realized at solar PV shares higher than 40%.

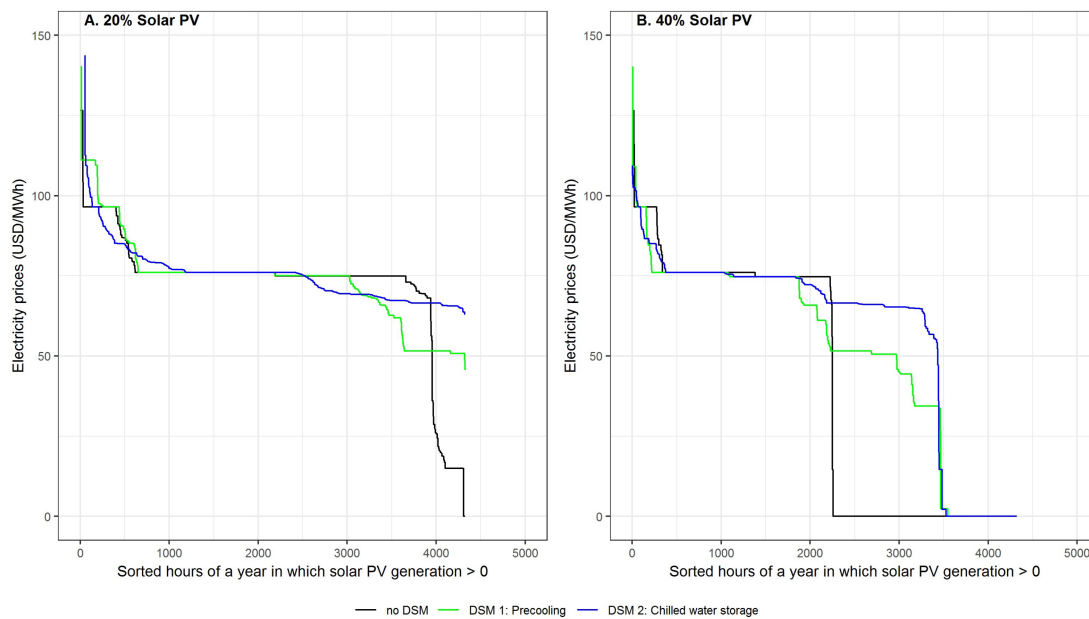


**Figure 8.** Duration curve of electricity prices as seen by solar PV plants 20% (left) and 40% (right) solar PV shares for the noDSM, Precooling, and CWS scenarios.

#### 4. Discussion and Conclusions

Managing electricity demand from air conditioners with precooling or chilled water storage reduces the impacts of solar PV variability (fluctuations due to weather and day/night cycles) and benefits the further adoption of solar PV generation. Both flexibility options can shift demand on diurnal time scales such that the challenges arising from the inflexibility of solar PV generation are strongly reduced. By shifting demand from evening to midday, both DSM options reduce the number of hours where PV generation sees very low or even zero market prices, and, accordingly, increases the revenues of PV plants.

For India, we found that, especially at solar PV shares above 40%, the economic value of solar PV in our modeling roughly doubled with demand flexibility, which increased the competitive and cost-optimal solar PV generation share at the assumed range of PV LCOE from 33–45% (without DSM) to ~45–60% (with DSM). Whereas the precooling of a building through simple programmable thermostats can already increase cost-optimal PV shares by ~7%, the longer storage period of chilled water tanks make this DSM option even more valuable for integrating PV, increasing the cost-optimal PV share by an additional 7%.

The economic value and, thus, the optimal shares depend on the assumed carbon price (here, 50 USD/t CO<sub>2</sub>). Increasing the carbon price would increase costs of carbon-intensive generators and would thus increase the cost-competitiveness of solar PV. Even without flexibility measures, carbon pricing can somewhat counteract the adverse economic impacts of variability by ruling out other options and without actually decreasing integration costs. However, at high PV shares, when curtailment is high and the capacity credit of solar PV is near zero, it would require very high CO<sub>2</sub> prices to incentivize an additional PV plant if no flexibility measures exist. In a system with both growing flexibility measures and carbon pricing, the economic value of solar PV can be stabilized and high shares of solar PV are likely cost-efficient.

Other competing flexibility options, such as electricity storage (especially batteries) or flexibility from newly electrified load (for electric vehicles, industrial or buildings' heat), can reduce the benefits of AC-related DSM. The main advantage of precooling and chilled water storage is that these are rather low-tech flexibility options with comparatively low costs. The main disadvantage of AC-related DSM might be that it is a very distributed and decentral source of flexibility and it requires a mature

electricity market with time-of-use or ideally real-time pricing for residential and commercial buildings to unlock the flexibility potential. Digitalization and new actors such as electricity aggregators and demand-side bidding mechanisms are likely to facilitate this transition.

In this paper, we focused on analyzing DSM without considering the interaction with batteries. Batteries can be installed independently of AC demand and are thus more flexible. Including this additional option (based on today's costs) would likely lead to batteries being deployed when AC-related DSM reaches its potential deployment limits.

Our insights are transferable to most regions with high solar irradiation in warm climate zones such as Africa, Asia, Latin America, and the Middle East, which make up about 70% of the world's population, while only a small share of the population currently own an AC (India: 4% of households). Both population and the adoption of ACs are projected to increase strongly, which benefits the demand-supply matching of solar PV and creates significant potential for AC-related demand flexibility by adding thermal storage. The synergies of AC and solar PV uptake have implications for policymakers, energy planners, regulators, and system operators. Considering this potentially massive and distributed source of flexibility can pave the way for a solar-heavy power supply for a major share of future electricity demand.

**Author Contributions:** A.M.E., R.P. and G.L. designed the study. A.M.E. conducted the modeling work, post-processing and created the figures. F.U. and R.P. supported interpreting the results and deriving conclusions. A.M.E. wrote the main part of the paper. F.U. and R.P. supported the writing. All authors have read and agreed to the published version of the manuscript.

**Funding:** This work was supported by the European Union's Horizon 2020 research and innovation program under grant agreement No 730403 (INNOPATHS) and by the German Federal Ministry of Education and Research (BMBF) in the START project (03EK3046A).

**Acknowledgments:** Previous works of this research have been presented at one of AME's Ph.D. seminars at PIK and at the "2nd International Conference on Large-Scale Grid Integration of Renewable Energy in India". We therefore thank the seminar and conference audiences for useful discussions and suggestions. We also thank Wolf-Peter Schill, Alexander Zerrahn and their colleagues for developing the basic DIETER model and for making it open source.

**Conflicts of Interest:** The authors declare no conflict of interest.

## Appendix A. Estimation of Hourly AC Demand

For the first step of the procedure to derive hourly total electricity demand, the estimation of hourly AC demand, we use an extended degree-day method similar to the one used by Gils (2014) [67] as comprehensive data on hourly AC demand in India does not exist. We start by estimating each day's share of the annual AC demand using that day's share of population-weighted cooling degree-days (CDDs) with a base temperature of 21 °C. Gridded daily ambient temperature and population data for India in 2010 is taken from the Inter-Sectoral Impact Model Intercomparison Project (ISIMIP) [68,69]. The daily AC demand modelling does not factor in the impact of humidity and the future growth of CDDs due to global warming. In addition, daily AC demand as estimated solely by CDDs might be overestimated for spring days, as AC demand is mainly concentrated in the summer [70]. Next, the daily AC demand is downscaled to hourly demand with the help of one representative daily AC demand shape. Evidence of aggregate daily AC demand profiles from India are not well documented in the literature. Faced with this lack of data, we resort to ERCOT's average weekday residential Central Air Conditioning (CAC) demand profile in peak season (May–September) from EPRI's Load Shape Library 5.0 [<http://loadshape.epri.com/enduse>], which peaks at 6 p.m., to represent the shape of daily AC demand curve in India in 2040. This choice is in line with the basic logic that as household incomes increase, AC usage becomes less cost-constrained: once an AC unit is installed, it is set to relatively constant temperatures because electricity costs make up a lower share of total income. Accordingly, as household income rises, AC power consumption grows increasingly related to temperature levels, mediated by building shell permeability and thermal mass, resulting in AC power demand peaking early in the evening, a few hours after peak temperatures (see Figure 2 in Stocker et al., 1980 [71]).

## Appendix B. Power Sector Modeling

**Table A1.** Locations of assumed wind farms for the calculation of hourly wind power yield.

State	Wind Farm Site	Latitude	Longitude
Tamil Nadu	Mupandal wind farm	8.25000	77.59000
Gujarat	Lamda Danida	21.91900	69.26300
Rajasthan	Jaisalmer Wind park	26.92000	70.90000
Andhra Pradesh	Beluguppa wind park	14.71528	77.13528
Maharashtra	Dhalgaon wind park	17.11722	74.98667
Karnataka	Acciona Tuppadahalli	13.91028	76.03056
Madhya Pradesh	Mamatkheda	23.33306	75.03583

**Table A2.** Technical and cost assumptions on conventional generators, developed based on information in in [15,58–64].

Parameter	Nuclear	Hard Coal	CCGT	OCGT	Unit
Efficiency	34.3	43	58	45.7	%
Carbon content	0	0.354	0.202	0.202	t/MWh
Overnight investment costs	5500	1580	700	400	USD/kW
Annual fixed costs	140	55	25	20	USD/kW
Variable O&M costs		-	-		USD/kWh
Load change costs up and down	50	30	20	15	USD/MW
Technical lifetime	40	35	25	25	Years
Interest rate	7	7	7	7	%
Maximum capacity factor	85	85	85	85	%
Maximum load change for reserves	4	6	8	15	% of capacity per minute

**Table A3.** Fuel and CO<sub>2</sub> prices

Fuel Type/ CO <sub>2</sub> Price	Value	Unit
Hard coal	14	USD/MWh-th
Gas	34	USD/MWh-th
Nuclear	3	USD/MWh-th
CO <sub>2</sub> price	50	USD/t CO <sub>2</sub>

**Table A4.** Technical and cost assumptions on DSM measures, developed based on information in [15,35,37,45,69].

Parameter	Precooling	CWS	Unit
Load shifting costs	1	1	USD/MWh
Overnight investment costs	30	100	USD/kW
Annual fixed costs	-	-	USD/kW
Interest rate	7	7	%
Technical lifetime	10	10	Years
Efficiency	70	90	%
DSM maximum duration	4	8	Hours
DSM recovery time	1	1	Hours
Maximum installable capacity	350,000	350,000	MW

## References

1. “Low Renewable Auction Prices in India—Aggressive Bids or Unrealistic Expectations?” IHS Markit, 30. 2019. Available online: <https://ihsmarkit.com/research-analysis/low-renewable-auction-prices-in-india.html> (accessed on 7 February 2020).

2. India Targets 500GW of Renewables by 2030: Official|Recharge. Recharge|Latest Renewable Energy News. Available online: <https://www.rechargenews.com/transition/india-targets-500gw-of-renewables-by-2030-official/2-1-628026> (accessed on 7 February 2020).
3. Lawrenz, L.; Xiong, B.; Lorenz, L.; Krumm, A.; Hosenfeld, H.; Burandt, T.; Löffler, K.; Oei, P.Y.; Von Hirschhausen, C. Exploring Energy Pathways for the Low-Carbon Transformation in India—A Model-Based Analysis. *Energies* **2018**, *11*, 3001. [[CrossRef](#)]
4. Gadre, R.; Anandarajah, G. Assessing the evolution of India’s power sector to 2050 under different CO<sub>2</sub> emissions rights allocation schemes. *Energy Sustain. Dev.* **2019**, *50*, 126–138. [[CrossRef](#)]
5. Anandarajah, G.; Gambhir, A. India’s CO<sub>2</sub> emission pathways to 2050: What role can renewables play? *Appl. Energy* **2014**, *131*, 79–86. [[CrossRef](#)]
6. McCollum, D.L.; Zhou, W.; Bertram, C.; De Boer, H.S.; Bosetti, V.; Busch, S.; Després, J.; Drouet, L.; Emmerling, J.; Fay, M.; et al. Energy investment needs for fulfilling the Paris Agreement and achieving the Sustainable Development Goals. *Nat. Energy* **2018**, *7*, 589–599. [[CrossRef](#)]
7. Ueckerdt, F.; Brecha, R.; Luderer, G. Analyzing major challenges of wind and solar variability in power systems. *Renew. Energy* **2015**, *81*, 1–10. [[CrossRef](#)]
8. Sivaram, V.; Kann, S. Solar Power Needs a More Ambitious Cost Target. *Nat. Energy* **2016**, *1*, 1–3. Available online: <https://www.nature.com/articles/nenergy201636> (accessed on 23 August 2018). [[CrossRef](#)]
9. Creutzig, F.; Agoston, P.; Goldschmidt, J.C.; Luderer, G.; Nemet, G.; Pietzcker, R.C. The underestimated potential of solar energy to mitigate climate change. *Nat. Energy* **2017**, *2*, 17140. [[CrossRef](#)]
10. Hu, J.; Harmsen, R.; Crijns-Graus, W.; Worrell, E.; van den Broek, M. Identifying barriers to large-scale integration of variable renewable electricity into the electricity market: A literature review of market design. *Renew. Sustain. Energy Rev.* **2018**, *81*, 2181–2195. [[CrossRef](#)]
11. Mills, A.D.; Wiser, R.H. Strategies to mitigate declines in the economic value of wind and solar at high penetration in California. *Appl. Energy* **2015**, *147*, 269–278. [[CrossRef](#)]
12. Hirth, L. The market value of variable renewables: The effect of solar wind power variability on their relative price. *Energy Econ.* **2013**, *38*, 218–236. [[CrossRef](#)]
13. Clò, S.; D’Adamo, G. The dark side of the sun: How solar power production affects the market value of solar and gas sources. *Energy Econ.* **2015**, *49*, 523–530. [[CrossRef](#)]
14. Hale, E.T.; Stoll, B.L.; Novacheck, J.E. Integrating solar into Florida’s power system: Potential roles for flexibility. *Sol. Energy* **2018**, *170*, 741–751. [[CrossRef](#)]
15. Deshmukh, R.; Callaway, D.; Abhyankar, N.; Phadke, A. Cost and Value of Wind and Solar in India’s Electric System in 2030. In Proceedings of the 1st International Conference on Large-Sale Integration of Renewable Energies in India, New Delhi, India, 6–8 September 2017; Available online: [https://regridintegrationindia.org/wp-content/uploads/sites/3/2017/09/8B\\_1\\_GIZ17\\_174\\_paper\\_Ranjit\\_Deshmukh.pdf](https://regridintegrationindia.org/wp-content/uploads/sites/3/2017/09/8B_1_GIZ17_174_paper_Ranjit_Deshmukh.pdf) (accessed on 26 July 2019).
16. Palchak, J.D.; Chernyakhovskiy, I.; Bowen, T.; Narwade, V. *India 2030 Wind and Solar Integration Study: Interim Report*; NREL/TP-6A20-73854; 1524771; National Renewable Energy Lab. (NREL): Golden, CO, USA, 2019. [[CrossRef](#)]
17. Chaturvedi, V.; Koti, P.N.; Ramakrishnan, A. Sustainable Development, Uncertainties, and India’s Climate Policy: Pathways towards Nationally Determined Contribution and Mid-Century Strategy. *CEEW*. 2018. Available online: [https://www.ceew.in/sites/default/files/CEEW\\_Sustainable\\_Development\\_Uncertainties\\_India\\_Climate\\_Policy\\_30Apr18.pdf](https://www.ceew.in/sites/default/files/CEEW_Sustainable_Development_Uncertainties_India_Climate_Policy_30Apr18.pdf) (accessed on 3 December 2019).
18. Wimmmler, C.; Hejazi, G.; Fernandes, E.D.; Moreira, C.; Connors, S. Impacts of Load Shifting on Renewable Energy Integration. *Energy Procedia* **2017**, *107*, 248–252. [[CrossRef](#)]
19. Braff, W.A.; Mueller, J.M.; Trancik, J.E. Value of storage technologies for wind and solar energy. *Nat. Clim. Chang.* **2016**, *6*, 964–969. [[CrossRef](#)]
20. Cheng, F.; Willard, S.; Hawkins, J.; Arellano, B.; Lavrova, O.; Mammoli, A. Applying battery energy storage to enhance the benefits of photovoltaics. In Proceedings of the 2012 IEEE Energytech, Cleveland, OH, USA, 29–31 May 2012; pp. 1–5. [[CrossRef](#)]
21. Castro, M.; Delgado, A.; Argul, F.J.; Colmenar, A.; Yeves, F.; Peire, J. Grid-connected PV buildings: Analysis of future scenarios with an example of Southern Spain. *Sol. Energy* **2005**, *79*, 86–95. [[CrossRef](#)]



22. Calise, F.; Cappiello, F.L.; d'Accadia, M.D.; Vicidomini, M. Dynamic simulation, energy and economic comparison between BIPV and BIPVT collectors coupled with micro-wind turbines. *Energy* **2020**, *191*, 116439. [[CrossRef](#)]
23. Bellocchi, S.; Manno, M.; Noussan, M.; Prina, M.G.; Vellini, M. Electrification of transport and residential heating sectors in support of renewable penetration: Scenarios for the Italian energy system. *Energy* **2020**, *196*, 117062. [[CrossRef](#)]
24. Brown, P.R.; O'Sullivan, F.M. Shaping photovoltaic array output to align with changing wholesale electricity price profiles. *Appl. Energy* **2019**, *256*, 113734. [[CrossRef](#)]
25. Ebrahimi, M. Storing electricity as thermal energy at community level for demand side management. *Energy* **2020**, *193*, 116755. [[CrossRef](#)]
26. Bloess, A.; Schill, W.-P.; Zerrahn, A. Power-to-heat for renewable energy integration: A review of technologies, modeling approaches, and flexibility potentials. *Appl. Energy* **2018**, *212*, 1611–1626. [[CrossRef](#)]
27. Ali, S.M.H.; Lenzen, M.; Huang, J. Shifting air-conditioner load in residential buildings: Benefits for low-carbon integrated power grids. *IET Renew. Power Gener.* **2018**, *12*, 1314–1323. [[CrossRef](#)]
28. Arteconi, A.; Hewitt, N.J.; Polonara, F. State of the art of thermal storage for demand-side management. *Appl. Energy* **2012**, *93*, 371–389. [[CrossRef](#)]
29. Levesque, A.; Pietzcker, R.C.; Baumstark, L.; de Stercke, S.; Grübler, A.; Luderer, G. How much energy will buildings consume in 2100? A global perspective within a scenario framework. *Energy* **2018**, *148*, 514–527. [[CrossRef](#)]
30. Isaac, M.; van Vuuren, D.P. Modeling global residential sector energy demand for heating and air conditioning in the context of climate change. *Energy Policy* **2009**, *37*, 507–521. [[CrossRef](#)]
31. Waite, M.; Cohen, E.; Torbey, H.; Piccirilli, M.; Tian, Y.; Modi, V. Global trends in urban electricity demands for cooling and heating. *Energy* **2017**, *127*, 786–802. [[CrossRef](#)]
32. Wenz, L.; Levermann, A.; Auffhammer, M. North–south polarization of European electricity consumption under future warming. *Proc. Natl. Acad. Sci. USA* **2017**, *114*, E7910–E7918. [[CrossRef](#)] [[PubMed](#)]
33. Jakubcionis, M.; Carlsson, J. Estimation of European Union residential sector space cooling potential. *Energy Policy* **2017**, *101*, 225–235. [[CrossRef](#)]
34. IEA. *The Future of Cooling*; International Energy Agency: Paris, France, 2018.
35. Phadke, A.; Abhyankar, N.; Shah, N. Avoiding 100 New Power Plants by Increasing Efficiency of Room Air Conditioners in India: Opportunities and Challenges. In Proceedings of the 7th International Conference on Energy Efficiency in Domestic Appliances and Lighting (EEDAL'13), Coimbra, Portugal, 11–13 September 2013.
36. Cole, W.J.; Rhodes, J.D.; Gorman, W.; Perez, K.X.; Webber, M.E.; Edgar, T.F. Community-scale residential air conditioning control for effective grid management. *Appl. Energy* **2014**, *130*, 428–436. [[CrossRef](#)]
37. Turner, W.J.N.; Walker, I.S.; Roux, J. Peak load reductions: Electric load shifting with mechanical pre-cooling of residential buildings with low thermal mass. *Energy* **2015**, *82*, 1057–1067. [[CrossRef](#)]
38. Yang, L.; Li, Y. Cooling load reduction by using thermal mass and night ventilation. *Energy Build.* **2008**, *40*, 2052–2058. [[CrossRef](#)]
39. Wolisz, H.; Harb, H.; Matthes, P.; Streblow, R.; Müller, D. Dynamic Simulation of Thermal Capacity and Charging/Discharging Performance for Sensible Heat Storage in Building Wall Mass. In Proceedings of the BS2013, Chambéry, France, 26–28 August 2013.
40. Nazari-Heris, M.; Kalavani, F. Evaluation of Peak Shifting and Energy Saving Potential of Ice Storage Based Air Conditioning Systems in Iran. *J. Oper. Autom. Power Eng.* **2017**, *5*, 163–170.
41. Lo, C.-C.; Tsai, S.-H.; Lin, B.-S. Ice Storage Air-Conditioning System Simulation with Dynamic Electricity Pricing: A Demand Response Study. *Energies* **2016**, *9*, 113. [[CrossRef](#)]
42. Deetjen, T.A.; Reimers, A.S.; Webber, M.E. Can storage reduce electricity consumption? A general equation for the grid-wide efficiency impact of using cooling thermal energy storage for load shifting. *Environ. Res. Lett.* **2018**, *13*, 024013. [[CrossRef](#)]
43. Hasnain, S.M. Review on sustainable thermal energy storage technologies, Part II: Cool thermal storage. *Energy Convers. Manag.* **1998**, *39*, 1139–1153. [[CrossRef](#)]
44. Sarbu, I.; Sebarchievici, C. A Comprehensive Review of Thermal Energy Storage. *Sustainability* **2018**, *10*, 191. [[CrossRef](#)]

45. Van Asselt, A.; Reindl, D.T.; Nellis, G.F. Policy recommendations for using cool thermal energy storage to increase grid penetration of renewable power sources (1607-RP). *Sci. Technol. Built Environ.* **2017**, *24*, 759–769. [CrossRef]
46. Deetjen, T.A.; Vitter, J.S.; Reimers, A.S.; Webber, M.E. Optimal dispatch and equipment sizing of a residential central utility plant for improving rooftop solar integration. *Energy* **2018**, *147*, 1044–1059. [CrossRef]
47. Goldenberg, C.; Dyson, M.; Masters, H. Demand Flexibility—The key to enabling a low-cost, low-carbon grid. *Rocky Mt. Inst.* **2018**, *13*, 6.
48. Zerrahn, A.; Schill, W.-P. A Greenfield Model to Evaluate Long-Run Power Storage Requirements for High Shares of Renewables. *SSRN J.* **2015**. [CrossRef]
49. Peppanen, J.; Reno, M.J.; Grijalva, S. Thermal energy storage for air conditioning as an enabler of residential demand response. In Proceedings of the 2014 North American Power Symposium (NAPS), Pullman, WA, USA, 7–9 September 2014; pp. 1–6.
50. Herter, K.; Okuneva, Y. SMUD’s 2012 Residential Precooling Study—Load Impact Evaluation. 2013. Available online: [http://www.herterenergy.com/pdfs/Publications/2013\\_Herter\\_SMUD\\_ResPrecooling.pdf](http://www.herterenergy.com/pdfs/Publications/2013_Herter_SMUD_ResPrecooling.pdf) (accessed on 9 February 2018).
51. Levesque, A.; Pietzcker, R.C.; Luderer, G. Halving energy demand from buildings: The impact of low consumption practices. *Technol. Forecast. Soc. Chang.* **2019**, *146*, 253–266. [CrossRef]
52. Operation Performance of Generating Stations in the Country during the Year 2010–2011—An Overview. CEA: New Delhi, India, 2011; Available online: [http://cea.nic.in/reports/annual/generationreview/generation\\_review-2010.pdf](http://cea.nic.in/reports/annual/generationreview/generation_review-2010.pdf) (accessed on 3 April 2020).
53. Boßmann, T.; Pfluger, B.; Wietschel, M. The shape matters! How structural changes in the electricity load curve affect optimal investments in generation capacity. In Proceedings of the 10th International Conference on the European Energy Market (EEM), Stockholm, Sweden, 28–30 May 2013; pp. 1–8.
54. Palchak, D.; Cochran, J.; Deshmukh, R.; Ehlen, A.; Soonee, R.; Narasimhan, S.; Joshi, M.; McBennett, B.; Milligan, M.; Sreedharan, P.; et al. *Greening the Grid: Pathways to Integrate 175 Gigawatts of Renewable Energy into India’s Electric Grid, National Study*; Lawrence Berkeley National Lab.(LBNL): Berkeley, CA, USA; National Renewable Energy Lab.(NREL): Golden, CO, USA; Power System Operation Corporation (POSOCO): New Delhi, India; US Agency for International Development (USAID): Washington, DC, USA, 2017; Volume 1.
55. *1.17-System Advisor Model (SAM), Version 2017*; NREL: Golden, CO, USA, 2017.
56. Palchak, D.; Cochran, J.; Deshmukh, R.; Ehlen, A.; Soonee, R.; Narasimhan, S.; Joshi, M.; McBennett, B.; Milligan, M.; Sreedharan, P.; et al. *Greening the Grid: Pathways to Integrate 175 Gigawatts of Renewable Energy into India’s Electric Grid*; NREL/TP-6A20-68530; 1369138; National Renewable Energy Lab.(NREL): Golden, CO, USA, 2017; Vol. I—National Study. [CrossRef]
57. Schneider, M.; Froggatt, A.; Hazemann, J.; von Hirschhausen, C.; Katsuta, T.; Wealer, B.; Lovins, A.B.; Ramana, M.V.; Stienne, A.; Friedhelm, M. The World Nuclear Industry Status Report 2019. A Mycle Scheider Consulting Project. 2019. Available online: <https://www.worldnuclearreport.org/IMG/pdf/wnisr2019-v2-hr.pdf> (accessed on 2 March 2020).
58. De Vita, A.; Kielichowska, I.; Mandatowa, P.; Capros, P.; Dimopoulou, E.; Evangelopoulou, S.; Fotiou, T.; Kannavou, M.; Siskos, P.; Zazias, G. *Technology Pathways in Decarbonisation Scenarios*; E3 Modelling; Tractebel: Brussels, Belgium, 2018.
59. Schröder, A.; Kunz, F.; Meiss, J.; Mendelevitch, R.; von Hirschhausen, C. Current and Prospective Costs of Electricity Generation until 2050. *DIW.* 2013. Available online: [https://www.diw.de/documents/publikationen/73/diw\\_01.c.424566.de/diw\\_datadoc\\_2013-068.pdf](https://www.diw.de/documents/publikationen/73/diw_01.c.424566.de/diw_datadoc_2013-068.pdf) (accessed on 5 April 2020).
60. International Energy Agency (IEA). *World Energy Outlook 2018*. 2018. Available online: <https://webstore.iea.org/world-energy-outlook-2018> (accessed on 24 June 2019).
61. *Projected Costs of Generating Electricity 2015 Edition*; IEA & NEA: Paris, France, 2015.
62. Ray, D. *Lazard’s Levelized Cost of Energy Analysis—Version 13.0*; Lazard: New York, NY, USA, 2019; p. 20.
63. Aboumahmoub, T.; Auer, C.; Bauer, N.; Baumstark, L.; Bertram, C.; Bi, S.; Dietrich, J.; Dirnacher, A.; Giannousakis, A.; Haller, M.; et al. REMIND—Regional Model of Investments and Development v2. *Zenodo* **2020**. [CrossRef]
64. Schill, W.-P.; Zerrahn, A. Long-run power storage requirements for high shares of renewables: Results and sensitivities. *Renew. Sustain. Energy Rev.* **2018**, *83*, 156–171. [CrossRef]

65. Zerrahn, A.; Schill, W.-P. Long-run power storage requirements for high shares of renewables: Review and a new model. *Renew. Sustain. Energy Rev.* **2017**, *79*, 1518–1534. [[CrossRef](#)]
66. Zerrahn, A.; Schill, W.-P. On the representation of demand-side management in power system models. *Energy* **2015**, *84*, 840–845. [[CrossRef](#)]
67. Gils, H.C. Assessment of the theoretical demand response potential in Europe. *Energy* **2014**, *67*, 1–18. [[CrossRef](#)]
68. Weedon, G.P.; Gomes, S.; Viterbo, P.; Shuttleworth, W.J.; Blyth, E.; Österle, H.; Adam, J.C.; Bellouin, N.; Boucher, O.; Best, M. Creation of the WATCH Forcing Data and Its Use to Assess Global and Regional Reference Crop Evaporation over Land during the Twentieth Century. *J. Hydrometeor.* **2011**, *12*, 823–848. [[CrossRef](#)]
69. Weedon, G.P.; Balsamo, G.; Bellouin, N.; Gomes, S.; Best, M.J.; Viterbo, P. The WFDEI meteorological forcing data set: WATCH Forcing Data methodology applied to ERA-Interim reanalysis data. *Water Resour. Res.* **2014**, *50*, 7505–7514. [[CrossRef](#)]
70. McMahon, J.E.; Chan, P.; Eto, J.; Koomey, J.; Levine, M.; Pignone, C.; Ruderman, H. The LBL Residential Energy and Hourly Demand Models. *Strateg. Plan. Energy Nat. Resour.* **1987**, 205–212.
71. Stocker, D.V. Load management study of simulated control of residential central air conditioners on the Detroit Edison Company System. *IEEE Trans. Power Appar. Syst.* **1980**, PAS-99, 1616–1624. [[CrossRef](#)]



© 2020 by the authors. Licensee MDPI, Basel, Switzerland. This article is an open access article distributed under the terms and conditions of the Creative Commons Attribution (CC BY) license (<http://creativecommons.org/licenses/by/4.0/>).